Supporting Information

Efficient organic manganese (II) bromide green-light-emitting diodes enabled by manipulating hole and electron transport layer

Atanu Jana[a], Vijaya Gopalan Sree[a], Qiankai Ba[b], Seong Chan Cho[c], Sang Uck Lee[c], Sangeun Cho[a], Yongcheol Jo[a], Abhishek Meena[a], Hyungsang Kim[a], and Hyunsik Im*[a]*

[a]Division of Physics and Semiconductor Science, Dongguk University, Seoul 04620, Republic of Korea

[b]Center for Superfunctional Materials, Department of Chemistry, School of Natural Science, Ulsan National Institute of Science and Technology (UNIST), 50 Unist-gil, Ulsan 44919, Korea

[c]Department of Applied Chemistry, Center for Bionano Intelligence Education and Research, Hanyang University, Ansan 15588, Republic of Korea

Physical Measurements

The powder X-ray diffraction (PXRD) was done using a D/MAX2500V/PC diffractometer, Rigaku using a Cu-rotating anode X-ray. The scan rate was 2 °/ minute. X-ray photoelectron spectra (XPS) were collected using the K-alpha model, ThermoFisher. Scanning electron microscopy (SEM) images were captured in SU8220 Cold FE-SEM, Hitach High-Technologies. Thermogravimetric analysis (TGA) was done using the Q500 model, TA.

The optical diffuse reflectance spectra solid samples were collected using a Cary 5000 UV-Vis-NIR Spectrophotometer, (Agilent) with an integrated sphere in diffuse-reflectance mode and then converted to Kubelka-Munk function, F(R). The photoluminescence (PL) and PL excitation (PLE) spectra were taken using Cary Eclipse fluorometer, (Varian) in solid-state. Photoluminescence quantum yield (PLQY) was measured in FP-8500ST Spectrofluorometer, (Jasco International). Time-resolved photoluminescence spectrum was done using NF900 (FLS920), (Edinburgh Instrument, UK). UPS analysis were measured by Nexsa XPS system (ThermoFisher Scientific, UK) (base pressure 2.0×10^{-7} Torr) (He I 21.2 eV), Korea basic science institute (KBSI), South Korea.

Crystal structure analysis

SC XRD analysis was conducted at the Korea Basic Science Institute (Seoul). Data were collected using a Bruker D8 Venture PHOTON 100 CMOS diffractometer equipped with a graphite-monochromated Mo Kα (λ = 0.7107 Å) radiation source at 25 °C. A light yellow crystal was immersed in paraton oil and mounted on the head of a KAPPA four-circle goniometer with φ, κ, ω, and 2θ axes, by which the crystal was rotated. The unit cell parameters were determined by collecting the diffracted intensities from 24 frames measured in two different crystallographic zones and using difference vectors. SMART APEX2 (Bruker, 2012) and SAINT (Bruker, 2012) were used for data collection and integration. The multi-scan method implemented in SADABS was used for absorption correction. Direct methods were used to resolve the crystal structure and refinement was conducted using full-matrix least-squares on F2 with SHELXTL. All of the non-hydrogen atoms were refined anisotropically, and the hydrogen atoms were added to their geometrically ideal positions. The CCDC number 2071564 was assigned to SC 1. [CCDC 2071564 contains the supplementary crystallographic data for this paper. These data can be obtained free of charge from the Cambridge Crystallographic Data Centre at www. ccdc.cam.ac.uk/data_request / cif.]

Device fabrication and characterization

ITO-coated glass substrates were sonicated in acetone, isopropyl alcohol, and deionized water and then dried under flowing N_2. The ITO films were then treated in a UV–ozone chamber for 20 min. PEDOT:PSS was then spin-coated at 4000 rpm for 30 s and annealed at 150 ℃ for 15 min in air. Organic layers were deposited on the PEDOT:PSS at a deposition rate of ≈0.3–0.7 Å s^{-1} and a pressure of 1 × 10^{-7} Torr, and the samples were then transported to a metal deposition chamber using robot arms. Lithium fluoride and aluminum were deposited at 1 × 10^{-7} Torr at deposition rates of 0.1 Å s^{-1} and 4 Å s^{-1}, respectively. The current density, voltage, and luminance characteristics were measured, and EL analysis was performed using a Keithley 2635A source meter and a CS2000 spectroradiometer (Konica Minolta). The EQE, CE, and PE were determined using an M6100 electrical analysis system (McScience). The structure of the fabricated devices was as follows:

The device structures of the fabricated devices are as follows;

Device 1 → ITO/PEDOT:PSS/TAPC/mCP (1) /TPBi/LiF/Al

Device 2 → ITO/PEDOT:PSS/TAPC/mCP:TPBi (1) TPBi/LiF/Al

Device 3 → ITO/PEDOT:PSS/TAPC/TCTA:TPBi (1) /TPBi/LiF/Al

Device 4→ ITO/PEDOT:PSS/TAPC/TCTA:TmPyPB (1) /TPBi/LiF/Al

Device 5 → ITO/PEDOT:PSS/TCTA/TCTA:TPBi (1) /TPBi/LiF/Al

Device 6 → ITO/PEDOT:PSS/NPB/TCTA:TPBi (1) /TPBi/LiF/Al

Device 7 → ITO/PEDOT:PSS/TPD/TCTA:TPBi (1) /TPBi/LiF/Al

Device 8 → ITO/PEDOT:PSS/TAPC/TCTA:TPBi (1) /BCP/LiF/Al

Device 9→ ITO/PEDOT:PSS/TAPC/TCTA:TPBi (1) /TmPyPB/LiF/Al

Device10→ITO/PEDOT:PSS/TPD/TAPC/TCTA:TPBi(1)/TmPyPB/LiF/Al

Density functional theory calculations

All electronic structure calculations were performed using density functional theory codes implemented in the Vienna Ab initio Simulation Package (VASP 5.4.4).[1–4] The projector augmented wave (PAW) method[3–6] was employed and exchange-correlation interactions were treated using the Perdew-Burke-Ernzerhof [7] functional under the generalized gradient approximation (GGA) by including Hubbard-U corrections (GGA+U). The value of Ueff = U-J was used for the Mn atoms for the treatment of the strong-correlation Mn-3d electrons.[8] The electron occupations were smeared with a Gaussian distribution function with a smearing width of 2 meV. The plane waves were incorporated until a high energy cut-off of 500 eV. We use the Monkhorst-Pack scheme to generate k-points with a reciprocal space resolution of $2\pi \times 0.05$ $Å^{-1}$.[9] Lattice constants and internal atomic positions were fully optimized until the residual forces were converged to within 0.04 eV/ Å .

Table S1. Crystal data and structure refinement for $[(H_2C=CHCH_2)(C_6H_5)_3P]_2MnBr_4$ (1) SC.

Empirical formula	C42 H40 Br4 Mn P2	
Formula weight	981.26	
Temperature	223(2) K	
Wavelength	0.71073 Å	
Crystal system	Monoclinic	
Space group	$P2_1/n$	
Unit cell dimensions	a = 15.053(6) Å	α= 90°.
	b = 17.194(9) Å	β = 110.032(13)°.
	c = 17.126(7) Å	γ = 90°.
Volume	4164(3) $Å^3$	
Z	4	
Density (calculated)	1.565 Mg/m^3	
Absorption coefficient	4.260 mm^{-1}	
F(000)	1948	
Crystal size	0.204 x 0.154 x 0.152 mm^3	
Theta range for data collection	1.957 to 28.294°.	
Index ranges	-14<=h<=20, -22<=k<=22, -22<=l<=22	
Reflections collected	56031	
Independent reflections	10300 [R(int) = 0.0606]	
Completeness to theta = 25.242°	99.9 %	
Absorption correction	Semi-empirical from equivalents	
Max. and min. transmission	0.7457 and 0.6328	
Refinement method	Full-matrix least-squares on F^2	
Data / restraints / parameters	10300 / 2 / 442	
Goodness-of-fit on F^2	1.055	
Final R indices [I>2sigma(I)]	R1 = 0.0697, wR2 = 0.1571	
R indices (all data)	R1 = 0.1331, wR2 = 0.1859	
Extinction coefficient	n/a	
Largest diff. peak and hole	1.792 and -0.998 $e.Å^{-3}$	

Table S2. Structural parameters of $[(H_2C{=}CHCH_2)(C_6H_5)_3P]_2MnBr_4$ (**1**).

Bond	Bond lengths [Å]	Bond angles	Measurement [°]
Mn(1)-Br(3)	2.5077(14)	Br(3)-Mn(1)-Br(4)	108.95(5)
Mn(1)-Br(4)	2.5079(14)	Br(3)-Mn(1)-Br(1)	105.90(5)
Mn(1)-Br(1)	2.5093(13)	Br(4)-Mn(1)-Br(1)	110.87(5)
Mn(1)-Br(2)	2.5164(13)	Br(3)-Mn(1)-Br(2)	111.25(5)
P(1)-C(13)	1.764(7)	Br(4)-Mn(1)-Br(2)	108.22(5)
P(1)-C(7)	1.786(5)	Br(1)-Mn(1)-Br(2)	111.62(5)
P(1)-C(1)	1.790(6)	C(13)-P(1)-C(7)	108.5(3)
P(1)-C(19)	1.819(7)	C(13)-P(1)-C(1)	110.2(3)
C(1)-C(2)	1.381(8)	C(7)-P(1)-C(1)	109.2(3)
C(1)-C(6)	1.395(8)	C(13)-P(1)-C(19)	111.4(4)
C(2)-C(3)	1.385(9)	C(7)-P(1)-C(19)	108.1(3)
C(2)-H(2)	0.9400	C(1)-P(1)-C(19)	109.3(3)
C(3)-C(4)	1.368(10)	C(2)-C(1)-C(6)	119.9(6)
C(3)-H(3)	0.9400	C(2)-C(1)-P(1)	119.8(5)
C(4)-C(5)	1.375(9)	C(6)-C(1)-P(1)	120.2(4)
C(4)-H(4)	0.9400	C(1)-C(2)-C(3)	120.2(6)
C(5)-C(6)	1.394(8)	C(1)-C(2)-H(2)	119.9
C(5)-H(5)	0.9400	C(3)-C(2)-H(2)	119.9
C(6)-H(6)	0.9400	C(4)-C(3)-C(2)	120.1(7)
C(7)-C(12)	1.373(8)	C(4)-C(3)-H(3)	119.9
C(7)-C(8)	1.386(9)	C(2)-C(3)-H(3)	119.9
C(8)-C(9)	1.372(10)	C(3)-C(4)-C(5)	120.4(6)
C(8)-H(8)	0.9400	C(3)-C(4)-H(4)	119.8
C(9)-C(10)	1.332(11)	C(5)-C(4)-H(4)	119.8
C(9)-H(9)	0.9400	C(4)-C(5)-C(6)	120.3(6)
C(10)-C(11)	1.382(11)	C(4)-C(5)-H(5)	119.8
C(10)-H(10)	0.9400	C(6)-C(5)-H(5)	119.8
C(11)-C(12)	1.376(9)	C(5)-C(6)-C(1)	119.0(5)
C(11)-H(11)	0.9400	C(5)-C(6)-H(6)	120.5
C(12)-H(12)	0.9400	C(1)-C(6)-H(6)	120.5
C(13)-C(14)	1.370(10)	C(12)-C(7)-C(8)	118.5(6)
C(13)-C(18)	1.394(9)	C(12)-C(7)-P(1)	120.3(5)
C(14)-C(15)	1.382(11)	C(8)-C(7)-P(1)	121.1(5)
C(14)-H(14)	0.9400	C(9)-C(8)-C(7)	119.7(7)
C(15)-C(16)	1.421(13)	C(9)-C(8)-H(8)	120.1
C(15)-H(15)	0.9400	C(7)-C(8)-H(8)	120.1
C(16)-C(17)	1.356(13)	C(10)-C(9)-C(8)	121.4(7)
C(16)-H(16)	0.9400	C(10)-C(9)-H(9)	119.3
C(17)-C(18)	1.349(11)	C(8)-C(9)-H(9)	119.3
C(17)-H(17)	0.9400	C(9)-C(10)-C(11)	120.2(7)
C(18)-H(18)	0.9400	C(9)-C(10)-H(10)	119.9
C(19)-C(20)	1.453(9)	C(11)-C(10)-H(10)	119.9
C(19)-H(19A)	0.9800	C(12)-C(11)-C(10)	119.1(7)
C(19)-H(19B)	0.9800	C(12)-C(11)-H(11)	120.5
C(20)-C(21)	1.309(11)	C(10)-C(11)-H(11)	120.5
C(20)-H(20)	0.9400	C(7)-C(12)-C(11)	121.0(7)
C(21)-H(21A)	0.9400	C(7)-C(12)-H(12)	119.5
C(21)-H(21B)	0.9400	C(11)-C(12)-H(12)	119.5
P(2)-C(40)	1.773(7)	C(14)-C(13)-C(18)	120.4(7)
P(2)-C(22)	1.780(6)	C(14)-C(13)-P(1)	121.5(5)
P(2)-C(28)	1.797(6)	C(18)-C(13)-P(1)	118.0(6)

P(2)-C(34)	1.809(6)	C(13)-C(14)-C(15)	120.7(9)
C(22)-C(27)	1.392(9)	C(13)-C(14)-H(14)	119.6
C(22)-C(23)	1.405(8)	C(15)-C(14)-H(14)	119.6
C(23)-C(24)	1.369(10)	C(14)-C(15)-C(16)	117.7(9)
C(23)-H(23)	0.9400	C(14)-C(15)-H(15)	121.1
C(24)-C(25)	1.386(11)	C(16)-C(15)-H(15)	121.1
C(24)-H(24)	0.9400	C(17)-C(16)-C(15)	119.9(8)
C(25)-C(26)	1.377(11)	C(17)-C(16)-H(16)	120.0
C(25)-H(25)	0.9400	C(15)-C(16)-H(16)	120.0
C(26)-C(27)	1.383(10)	C(18)-C(17)-C(16)	122.0(9)
C(26)-H(26)	0.9400	C(18)-C(17)-H(17)	119.0
C(27)-H(27)	0.9400	C(16)-C(17)-H(17)	119.0
C(28)-C(33)	1.371(9)	C(17)-C(18)-C(13)	119.0(9)
C(28)-C(29)	1.388(9)	C(17)-C(18)-H(18)	120.5
C(29)-C(30)	1.391(10)	C(13)-C(18)-H(18)	120.5
C(29)-H(29)	0.9400	C(20)-C(19)-P(1)	115.8(6)
C(30)-C(31)	1.379(12)	C(20)-C(19)-H(19A)	108.3
C(30)-H(30)	0.9400	P(1)-C(19)-H(19A)	108.3
C(31)-C(32)	1.357(12)	C(20)-C(19)-H(19B)	108.3
C(31)-H(31)	0.9400	P(1)-C(19)-H(19B)	108.3
C(32)-C(33)	1.366(10)	H(19A)-C(19)-H(19B)	107.4
C(32)-H(32)	0.9400	C(21)-C(20)-C(19)	123.6(9)
C(33)-H(33)	0.9400	C(21)-C(20)-H(20)	118.2
C(34)-C(39)	1.382(9)	C(19)-C(20)-H(20)	118.2
C(34)-C(35)	1.383(10)	C(20)-C(21)-H(21A)	120.0
C(35)-C(36)	1.382(10)	C(20)-C(21)-H(21B)	120.0
C(35)-H(35)	0.9400	H(21A)-C(21)-H(21B)	120.0
C(36)-C(37)	1.357(12)	C(40)-P(2)-C(22)	110.1(3)
C(36)-H(36)	0.9400	C(40)-P(2)-C(28)	108.7(3)
C(37)-C(38)	1.383(13)	C(22)-P(2)-C(28)	109.3(3)
C(37)-H(37)	0.9400	C(40)-P(2)-C(34)	110.3(3)
C(38)-C(39)	1.386(10)	C(22)-P(2)-C(34)	109.4(3)
C(38)-H(38)	0.9400	C(28)-P(2)-C(34)	109.1(3)
C(39)-H(39)	0.9400	C(27)-C(22)-C(23)	118.5(6)
C(40)-C(41)	1.322(8)	C(27)-C(22)-P(2)	120.7(5)
C(40)-H(40A)	0.9800	C(23)-C(22)-P(2)	120.7(5)
C(40)-H(40B)	0.9800	C(24)-C(23)-C(22)	119.6(6)
C(41)-C(42)	1.445(10)	C(24)-C(23)-H(23)	120.2
C(41)-H(41)	0.9400	C(22)-C(23)-H(23)	120.2
C(42)-H(42A)	0.9400	C(23)-C(24)-C(25)	121.4(7)
C(42)-H(42B)	0.9400	C(23)-C(24)-H(24)	119.3
		C(25)-C(24)-H(24)	119.3
		C(26)-C(25)-C(24)	119.4(7)
		C(26)-C(25)-H(25)	120.3
		C(24)-C(25)-H(25)	120.3
		C(25)-C(26)-C(27)	119.9(8)
		C(25)-C(26)-H(26)	120.1
		C(27)-C(26)-H(26)	120.1
		C(26)-C(27)-C(22)	121.0(7)
		C(26)-C(27)-H(27)	119.5
		C(22)-C(27)-H(27)	119.5
		C(33)-C(28)-C(29)	119.8(6)
		C(33)-C(28)-P(2)	121.0(5)
		C(29)-C(28)-P(2)	119.2(5)

	C(28)-C(29)-C(30)	118.9(7)
	C(28)-C(29)-H(29)	120.5
	C(30)-C(29)-H(29)	120.5
	C(31)-C(30)-C(29)	119.9(8)
	C(31)-C(30)-H(30)	120.1
	C(29)-C(30)-H(30)	120.1
	C(32)-C(31)-C(30)	120.4(7)
	C(32)-C(31)-H(31)	119.8
	C(30)-C(31)-H(31)	119.8
	C(31)-C(32)-C(33)	120.2(8)
	C(31)-C(32)-H(32)	119.9
	C(33)-C(32)-H(32)	119.9
	C(32)-C(33)-C(28)	120.7(7)
	C(32)-C(33)-H(33)	119.6
	C(28)-C(33)-H(33)	119.6
	C(39)-C(34)-C(35)	121.2(7)
	C(39)-C(34)-P(2)	118.2(6)
	C(35)-C(34)-P(2)	120.6(5)
	C(36)-C(35)-C(34)	119.4(8)
	C(36)-C(35)-H(35)	120.3
	C(34)-C(35)-H(35)	120.3
	C(37)-C(36)-C(35)	119.8(9)
	C(37)-C(36)-H(36)	120.1
	C(35)-C(36)-H(36)	120.1
	C(36)-C(37)-C(38)	121.0(8)
	C(36)-C(37)-H(37)	119.5
	C(38)-C(37)-H(37)	119.5
	C(37)-C(38)-C(39)	120.1(8)
	C(37)-C(38)-H(38)	120.0
	C(39)-C(38)-H(38)	120.0
	C(34)-C(39)-C(38)	118.3(8)
	C(34)-C(39)-H(39)	120.8
	C(38)-C(39)-H(39)	120.8
	C(41)-C(40)-P(2)	123.7(6)
	C(41)-C(40)-H(40A)	106.4
	P(2)-C(40)-H(40A)	106.4
	C(41)-C(40)-H(40B)	106.4
	P(2)-C(40)-H(40B)	106.4
	H(40A)-C(40)-H(40B)	106.5
	C(40)-C(41)-C(42)	123.9(7)
	C(40)-C(41)-H(41)	118.1
	C(42)-C(41)-H(41)	118.1
	C(41)-C(42)-H(42A)	120.0
	C(41)-C(42)-H(42B)	120.0
	H(42A)-C(42)-H(42B)	120.0

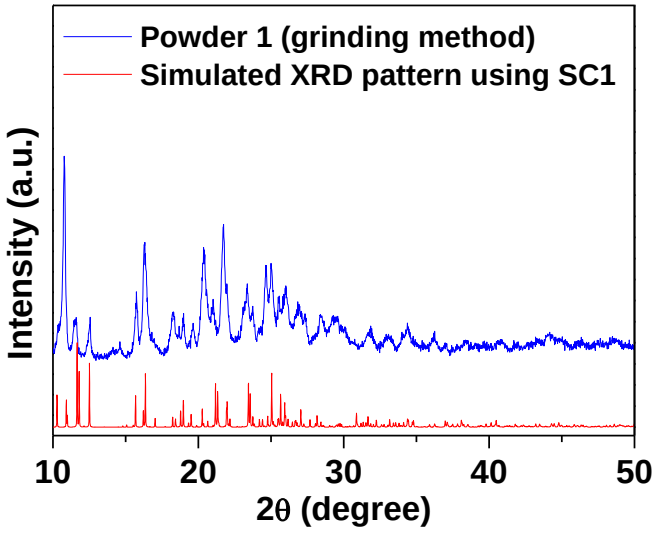

Figure S1. XRD results for the powdered form of **1** synthesized using a grinding method and simulated XRD patterns for the SC form of **1**.

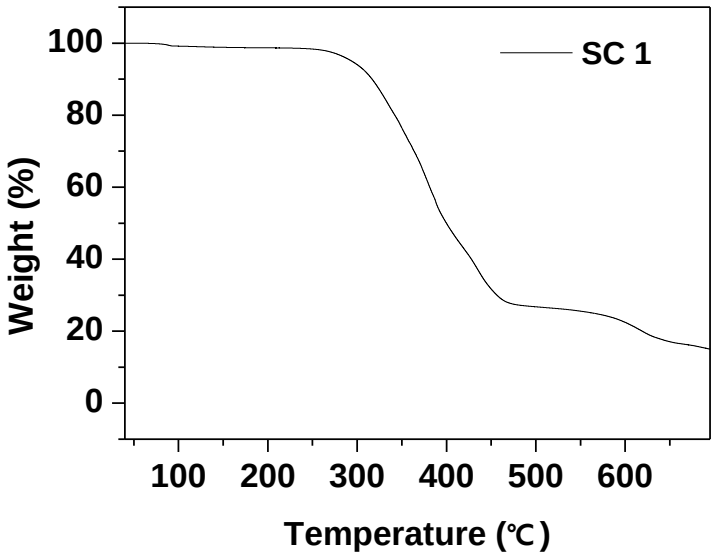

Figure S2. Thermogravimetric analysis of **1**.

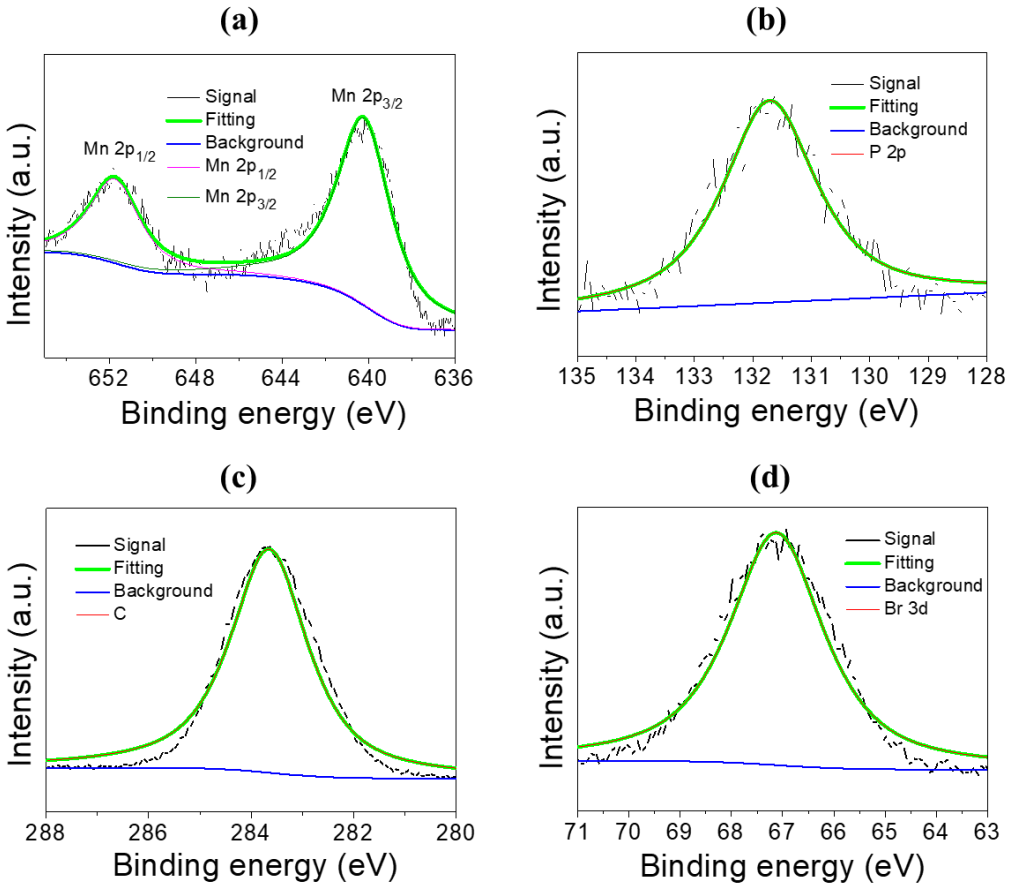

Figure S3. XPS analysis for **1**. XPS results for (a) Mn, (b) P, (c) C, and (d) Br.

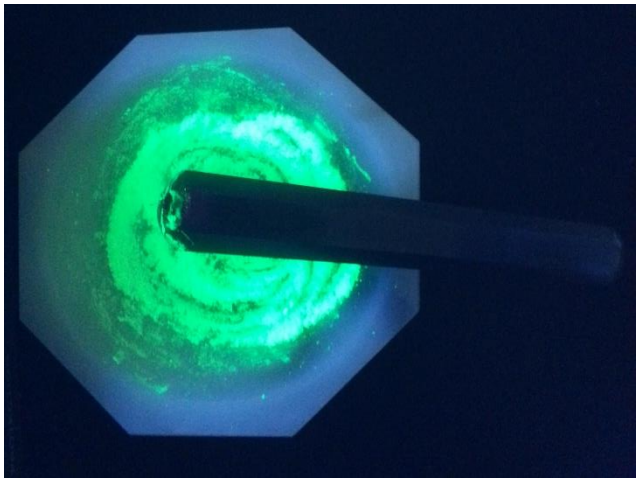

Figure S4. Synthesis of **1** using mechanochemical grinding. The synthesized product exhibited bright green fluorescence under UV light.

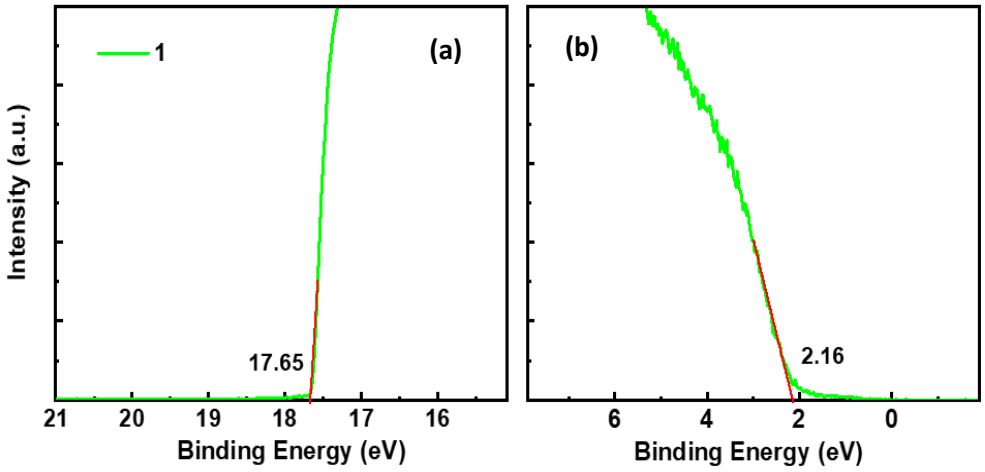

Figure S5. UPS spectra showing a) secondary cut-off and b) valance band region of **1**. UPS is usually used to determine the Fermi level (E_F) and the valence band maximum with respect to vacuum level. The work function (Φ) is determined by the difference between the incident photon energy (21.22 eV) and the binding energy of the secondary electron cut-off ($\Phi = 21.22 - (E_{cut\text{-}off} - E_F)$).[10]

Table S3. Energy Gap and HOMO/LUMO Energy Level for $[(H_2C{=}CHCH_2)(C_6H_5)_3P]_2MnBr_4$ (**1**).

Complex	ΔE_g[a] / eV	HOMO[b]/ eV	LUMO[c]/ eV
$[(H_2C{=}CHCH_2)(C_6H_5)_3P]_2MnBr_4$ (**1**)	2.6	5.7	3.1

a) Calculated from the onset wavelength of the absorption spectrum.

b) Calculated from UPS.

c) Determined using the HOMO energy level and E_g. LUMO = HOMO – ΔE_g

Table S4: Comparison of turn on voltage and brightness for organic-inorganic hybrid Mn(II)-based green-light-emitting PHOLEDs published to date.

Mn-based LEDs	V_{on} [V]	Brightness (cd m^{-2})	Ref.
$(Ph_4P)_2[MnBr_4]$ Tetraphenylphosphonium (Ph_4P)	4.8	2339	Adv. Mater. **2017**, 29, 1605739
DBFDPO-$MnBr_2$ 4,6-Bis(diphenylphosphoryl) dibenzofuran (DBFDO)	3.1	889	Adv. Optical Mater. **2019**, 7, 1801160
$[(H_2C{=}CHCH_2)(C_6H_5)_3P]_2MnBr_4$ Allyltriphenylphosphonium $[(H_2C{=}CHCH_2)(C_6H_5)_3P]$	3	4885	Our work, 2021

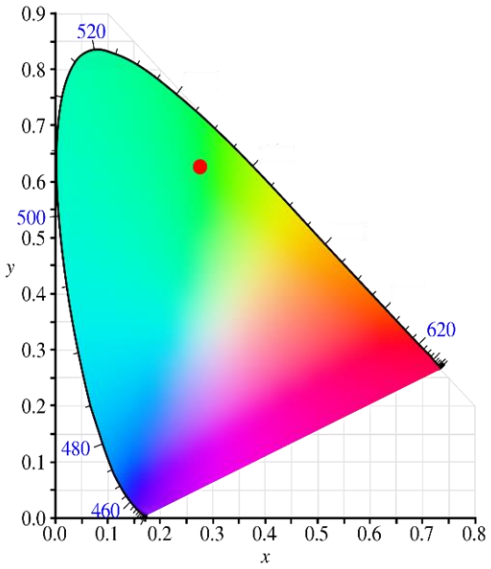

Figure S6. CIE chromaticity diagram for Device 10.

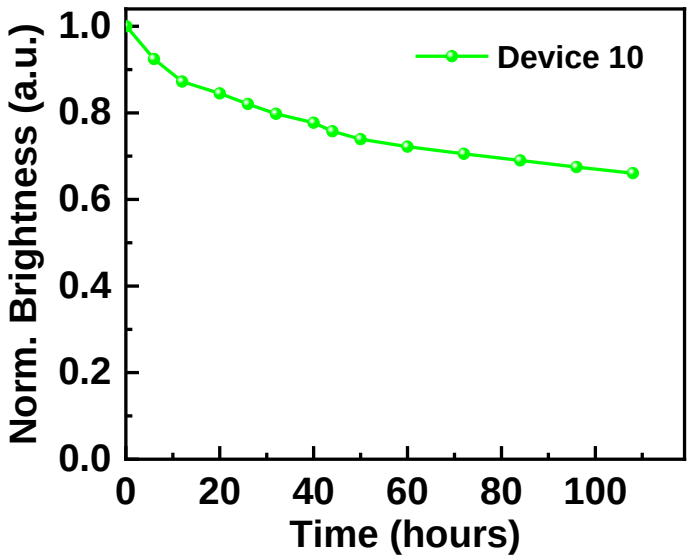

Figure S7. Device lifetime for the PHOLED device 10.

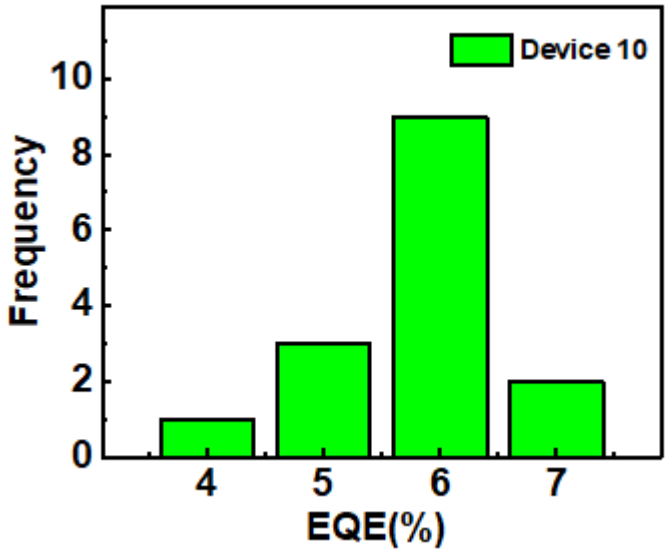

Figure S8. EQE distribution for the PHOLED devices (Device 10).

Table S5: Electroluminescent performance of the solution processed PHOLED device.

	Voltage (V)		Luminance (cd/m^2)	EQE (%)		CE (x,y)	
	V_{on}	At 100 cd/m^2	Max.	Max.	@ 30 mA/cm^2	Max.	@30 mA/cm^2
Soln.	**4.2**	**5.8**	**1301**	**3.77**	**2.91**	**8.35**	**6.33**

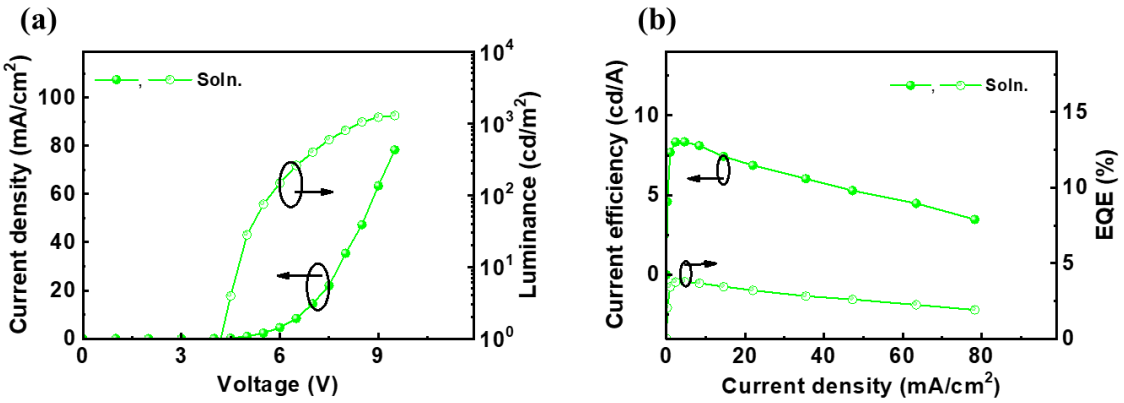

Figure S9. Characteristics of the solution processed PHOLED (Device Soln.: ITO/ PEDOT:PSS/TAPC/TCTA:TPBi(Mn(II))/TmPyPB/LiF/Al). (a) *J*–V–L curves. (b) CE/EQE vs. luminance of the solution processed PHOLED.

References

1 G. Kresse and J. Hafner, *Phys. Rev. B*, 1993, **48**, 13115–13118.

2 G. Kresse and J. Hafner, *Phys. Rev. B*, 1994, **49**, 14251–14269.

3 G. Kresse and J. Furthmüller, *Comput. Mater. Sci.*, 1996, **6**, 15–50.

4 G. Kresse and J. Furthmüller, *Phys. Rev. B*, 1996, **54**, 11169–11186.

5 P. E. Blöchl, *Phys. Rev. B*, 1994, **50**, 17953–17979.

6 G. Kresse and D. Joubert, *Phys. Rev. B*, 1999, **59**, 1758–1775.

7 J. P. Perdew, K. Burke and M. Ernzerhof, *Phys. Rev. Lett.*, 1996, **77**, 3865–3868.

8 T. A. Mellan, F. Corà, R. Grau-Crespo and S. Ismail-Beigi, *Phys. Rev. B*, 2015, **92**, 085151.

9 L. Vinet and A. Zhedanov, *J. Phys. A Math. Theor.*, 2011, **44**, 085201.

10 C. M. Chuang, P. R. Brown, M. G. Bawendi, U. States, U. States, C. Science, U. States and U. States, *Nat Mater.*, 2014, **13**, 796–801.